

# Study on Strength Characteristic of Unsaturated Undisturbed Lateritic Clay

Pan Jin<sup>1</sup>, Wenzhan Zhen<sup>2</sup>, Bo Chen<sup>1,\*</sup>, Youcheng Zhai<sup>1</sup>

<sup>1</sup> College of Civil Engineering and Architecture, Quzhou University, Zhejiang, China

<sup>2</sup> China Railway Eryuan Engineering Group Co. LTD, Sichuan, China

\*Corresponding Author.

## **Abstract:**

To investigate the effect of suction on strength characteristic of undisturbed lateritic clay, obtained from Jinhua-Quzhou Basin, the suction-controlled triaxial compression tests were carried out on undisturbed specimens under different suctions and net confining pressures, respectively. The obtained results show that the peak strength continues to increase with an increase in suction. Meanwhile, the stress-strain curves vary from strain-hardening to strain-soften for specimens gradually with an increase in suction. Correspondingly, the failure mode changes progressively from plastic failure with barrel deformation to brittle failure with localized deformation gradually. The variations of cohesion and internal friction angle with suction indicate that the cohesion increases linearly and nonlinearly with suction in semi-logarithmic coordinate before and after threshold suction (suction corresponding to abrupt change in variation tendency). On the contrary, the internal friction angle is almost the same with increasing suction before the threshold suction, while it increases significantly when the suction exceeds the threshold suction. Then, mercury intrusion porosimetry (MIP) was carried out to obtain pore size distributions (PSDs) of specimens with different suctions, to investigate the mechanism about the variations of strength parameters (cohesion and internal friction angle) with increasing suction. The MIP results indicate that typical unimodal PSDs exhibit in undisturbed lateritic clay. The peak of pore size distribution declines with an increase in suction, while the distributions of micro-pores are not affected by increasing suction. Moreover, the delimiting suction (suction corresponding to the delimiting diameter of macro- and micro-pores) calculated from the PSDs, is consistent to the threshold suction deduced from triaxial compression tests. Consequently, it can speculate that the different mechanism of suction effects on cohesion and internal friction angle, can be attributed to the fact that the cohesion is mainly influenced by the capillary water distributed in macro-pores, while the internal friction angle is mainly affected by the bound water distributed in micro-pores.

**Keywords:** *Undisturbed lateritic clay, Triaxial compression tests, Strength characteristic, Threshold suction, Pore size distribution.*

## I. INTRODUCTION

The lateritic clay, as a red or brown red clay with high plastic, is formed from the weathered products of carbonate rocks with laterization in warm and humid climate [1-2]. It is widely distributed in the tropical and sub-tropical regions in the world [3-7], and it is classified as a special clay owing to obvious cracks and shrinkage. Moreover, numerous geological hazards and accidents had been occurred in recent years, attributed to its undesirable geological characteristics [3,8,9]. In fact, many researchers had paid great attention to investigate the complex physical and mechanical behaviors of lateritic clay, including the disintegration characteristics, water retention behaviors and mechanical behaviors [2,5-7,10], and many beneficial conclusions had been obtained from experimental and theoretical investigations. In addition, the reported findings show that the mechanism about the effect of suction, soil structure, initial gravimetric water content on hydraulic and mechanical behaviors of lateritic clay, can be well illustrated by their different microstructure, i.e., the pore size distributions (PSDs)[5,7,10].

Reviewing the literatures about shear strength of unsaturated lateritic clay, it indicates that most of findings on their strength characteristics are mainly focus on the effect of initial gravimetric water content, dry density and wetting-drying cycle on the shear strength of lateritic clay. For example, Fu et al. [11] carried out direct shear tests on compacted specimens with the different initial gravimetric water contents, and the variations of cohesion and internal friction angle with initial gravimetric water content were obtained from the tests. Li et al. [12] also carried out direct shear tests on undisturbed specimens to investigate the variations of cohesion and internal friction angle with dry density. Zhang et al. [13] reveals the internal relationship between shear strength and number of drying and wetting cycles, by direct shear tests on compacted specimens with different wetting-drying cycles. In addition, Ng et al. [7] performed triaxial compression tests to investigate the effects of matric suction and net confining pressure on mechanical behavior of compacted specimens of lateritic clay with low suctions ( $s < 0.5$  MPa).

The current research status indicates that the tests to investigate shear strength of lateritic clay, were mainly carried out by direct shear apparatus. A little triaxial compression results of lateritic clay, are only obtained from specimens with low suctions, attributed to the limitation on air entry value of ceramic [7,14]. Indeed, the lateritic clay in shallow slopes is often in a state of high suction at arid summer, due to poor water retention behavior [2, 5, 10]. Meanwhile, the differences in existence of pore water and interaction between soil particles for specimens with low and high suctions, result in obvious different strength characteristic of unsaturated soil [15,16]. Therefore, it is necessary to investigate the shear strength of lateritic clay over a wide

suction range. Fortunately, with the mature of vapor equilibrium technique (VET) to control high suction[17], and high suction is only dependent on the gravimetric water content, not dependent on the dry density[18,19]. It is feasible to investigate the variations of shear strength and its parameters (cohesion and internal friction angle) with suction over a wide suction range, by the suction-controlled triaxial compression tests.

In addition, most unsaturated triaxial compression tests were carried out on compacted specimens of lateritic clay [7, 20], due to the difficulty of shaping triaxial specimens for undisturbed lateritic clay. However, the lateritic clay in the natural slopes is in an undisturbed state with long-term deposition, as well as the difference in hydraulic and mechanical behaviors between the undisturbed and compacted specimens is significant [5, 20]. As a result, it is worth carrying out triaxial compression test on undisturbed specimens of lateritic clay, to investigate the variations of shear strength and strength parameters (cohesion and internal friction angle) with suction over a wide suction range. Furthermore, the intrinsic mechanism about the suction effect on shear strength parameters of undisturbed lateritic clay, is needed to be further discussed upon the evolution of microstructure with increasing suction.

In this paper, the suction-controlled triaxial compression tests were carried out on undisturbed specimens with different suctions, under different net confining pressures. The variations of shear strength and strength parameters (cohesion and internal friction angle) with suction over a wide suction range, were illustrated according to obtained test results. Meanwhile, the mechanism about the effect of suction on the strength parameters was further discussed, upon the evolution of pore size distributions (PSDs) with increasing suction, obtained from the mercury intrusion porosimetry (MIP).

## **II. Specimens preparation and experimental program**

### **2.1 Tested material**

The undisturbed specimens used in the tests were obtained in the suburb of Quzhou city, a city located about 200 km from Hangzhou, the capital of Zhejiang Province (Fig 1). To obtain the high quality samples of natural lateritic clay, the block sampling method was employed to reduce the disturbance during the sampling, e.g., the block undisturbed samples (cubes with sides of 20 cm) were excavated about 1.5m below the surface, and they were sealed by plastic wrap and paraffin in the sampling site immediately, to prevent the loss of initial gravimetric water content of natural lateritic clay. Then, the block samples were delivered to laboratory carefully, and they are used to carry out the experimental investigation.



Fig 1: sampling site of tested lateritic clay

The basic physical properties (specific gravity, initial gravimetric water content, grain size distribution, free swell ratio, etc.) of the lateritic clay, were obtained according to ASTM [21], and the detailed data are summarized in Table I. In addition, the X-ray diffraction (XRD) result indicates that the main minerals are kaolinite, illite and vermiculite, as well as small amount of montmorillonite in the tested clay. The result of X-ray fluorescence (XRF) illustrates that the main chemical constituents of the tested clay are silicon dioxide ( $\text{SiO}_2$ ), aluminum sesquioxide ( $\text{Al}_2\text{O}_3$ ) and iron sesquioxide ( $\text{Fe}_2\text{O}_3$ )

## 2.2 Specimen preparation and suction equilibrium

The undisturbed triaxial specimens (diameter of 38.0 mm and height of 76.0 mm), were shaped from block samples of lateritic clay carefully. With the objective to investigate the effect of suction on the shear strength over a wide suction range, the suctions in specimens were applied by combing axial translation technique (ATT) and VET[5,15]. The low to medium suctions ( $s \leq 1.5$  MPa) in specimens were applied by the ATT, i.e., the triaxial specimens were placed on the high air-entry ceramic disk (15 bars) in pressure plate apparatus (Fig 2), and the targeted suctions can be imposed after the equilibrium of water and deformation reached by applying targeted air pressure[22]. Meanwhile, the high suctions ( $s > 1.5$  MPa) in specimens were applied by the VET, i.e., the triaxial specimens were sealed in desiccators with different saturated salt solutions at 20°C (Fig 3), and high suctions in specimens were imposed after the equilibrium of vapor potential between the specimens and saturated salt solution in desiccators. The detailed

saturated salt solutions and corresponding suctions [23] used in the tests are shown in Table II.

**Table I. Basic physical property of tested lateritic clay**

Physical property	Value	Grain size distribution	
Specific gravity	2.73	Sand (%)	15.7
Liquid limit (%)	41.1	Silty (%)	39.4
Plastic limit (%)	18.5	Clay (%)	44.9
Initial water content (%)	18.2-	Swelling and shrinkage	
	22.7		
Initial void ratio	0.70-	Free swelling ratio (%)	28.0
	0.78		
Maximum dry density (g/cm <sup>3</sup> )	1.68	Volumetric shrinkage	10.0
		(%)	
Optimum water content (%)	17.9	Linear shrinkage (%)	4.3

**Table II. Saturated salt solution and corresponding suction**

Saturated salt solution	RH/%	Total suction(MPa)
LiBr	6.6	367.5
NaCl	75.5	38.0
K <sub>2</sub> SO <sub>4</sub>	97.6	3.29



Fig 2: Pressure plate apparatus used in the ATT



Fig 3: Desiccator used in the VET

### 2.3 Suction-controlled triaxial tests

The eight suctions ( $s=0, 0.1, 0.2, 0.4, 1.2, 3.29, 38.0, 367.5$  MPa) and three net confining pressures ( $\sigma_m=0.1, 0.2, 0.4$ MPa) were used in suction-controlled triaxial tests on the undisturbed specimens. The detailed procedures of triaxial compression test were introduced as

follows. 1) the specimen with targeted suction was installed on GDS unsaturated triaxial apparatus. 2) the targeted net confining pressure was applied until water drainage and volume variation of specimen were less than  $100 \text{ mm}^3$  and  $200 \text{ mm}^3$  in 24 hours, respectively. 3) after reaching the equilibrium of water and deformation under net confining pressure, the specimen was sheared at axial strain rate of  $0.17 \text{ mm/h}$  to ensure the excess pore water pressure dissipated completely during the shear.

The water drainage and volumetric variation of specimen during processes of consolidation and shear under constant suction and net confining pressure, can be measured by transducers in GDS unsaturated triaxial apparatus. Meanwhile, the mass weight, total volume and gravimetric water content of specimen, can be determined easily at the stages of initial state and suction equilibrium. Consequently, the gravimetric water content, saturation degree and void ratio of tested specimen at different stages, can be determined by the variations of water and volume of specimen during the tests. The detailed information is summarized in Table III.

It is worth noting that suction can only be strictly controlled for specimens with low suctions during the consolidation and shear, attributed to the limitation on the air-entry value of ceramic disk in unsaturated triaxial apparatus ( $s \leq 0.5 \text{ MPa}$ ). For specimens with medium suctions ( $0.5 < s \leq 1.5 \text{ MPa}$ ) or high suctions ( $s > 1.5 \text{ MPa}$ ), controlling suction constant during the consolidation and shear, can be realized by keeping the gravimetric water content unchanged. It is because the suction is only dependent to gravimetric water content of specimen at medium to high suctions [19, 20]. Thus, the suction-controlled triaxial compression tests on specimens with medium or high suctions, can be replaced by exhaust undrained compression tests, and the round rubber membrane was placed on ceramic disk to maintain the gravimetric water content constant in tested specimen during consolidation and shear.

**Table III. Gravimetric water content, saturation degree and void ratio of specimens at different stages**

No.	Suction (MPa)	Net confining pressure (MPa)	Initial state			Equilibrium of suction			Equilibrium of net confining pressure		
			$w_0(\%)$	$S_{r0}(\%)$	$e_0$	$w_e(\%)$	$S_{re}(\%)$	$e_e$	$w_c(\%)$	$S_{rc}(\%)$	$e_c$
1	0	0.1	19.19	68.2	0.768	29.11	99.7	0.797	25.63	100	0.700
2	0	0.2	21.11	74.2	0.777	28.85	99.9	0.788	23.84	100	0.651



3	0	0.4	22.6 8	79.5	0.77 9	29.16	97.9	0.81 3	21.0 3	100	0.574
4	0.1	0.1	21.4 1	78.9	0.74 1	20.62	77.0	0.73 1	20.4 9	82.9	0.675
5	0.1	0.2	19.7 2	73.7	0.73 0	19.53	73.3	0.72 7	19.0 6	84.1	0.619
6	0.1	0.4	19.1 6	74.3	0.70 4	18.70	74.1	0.68 9	18.2 2	87.7	0.567
7	0.2	0.1	21.2 3	81.4	0.71 2	19.28	78.6	0.67 0	18.3 7	80.5	0.623
8	0.2	0.2	19.5 3	70.7	0.75 4	18.72	69.7	0.73 3	18.1 5	78.8	0.629
9	0.2	0.4	20.3 2	79.4	0.69 9	18.66	74.6	0.68 3	17.6 1	83.9	0.573
10	0.4	0.1	18.9 8	68.6	0.75 5	17.59	67.0	0.71 7	17.1 0	68.3	0.684
11	0.4	0.2	20.2 3	76.6	0.72 1	17.10	68.3	0.68 3	16.1 6	69.7	0.633
12 *	0.4	0.36	19.9 2	74.8	0.72 7	17.34	69.5	0.68 1	16.0 1	70.1	0.623
13	1.2	0.1	19.3 2	75.2	0.70 1	15.14	62.2	0.66 4	15.1 4	67.1	0.616
14	1.2	0.2	19.4 1	73.0	0.72 6	15.04	62.5	0.65 7	15.0 5	67.6	0.608
15	1.2	0.4	19.6 1	74.8	0.71 6	15.44	62.6	0.67 3	15.4 4	68.3	0.617
16	3.29	0.1	20.7 3	78.9	0.71 7	12.45	55.8	0.60 9	12.4 5	58.8	0.578
17	3.29	0.2	20.2 5	76.3	0.72 5	12.24	54.3	0.61 5	12.2 4	59.1	0.565
18	3.29	0.4	19.7 8	74.3	0.72 7	11.78	48.9	0.65 8	11.7 8	55.3	0.582
19	38.0	0.1	20.0 8	75.7	0.72 4	5.85	25.8	0.62 0	5.85	27.6	0.578
20	38.0	0.2	20.5 1	77.8	0.72 0	5.44	22.8	0.65 0	5.44	25.3	0.586
21	38.0	0.4	20.2 8	76.9	0.72 0	5.56	25.2	0.60 3	5.55	28.0	0.541
22	367.5	0.1	20.6 0	77.0	0.73 1	2.69	11.1	0.66 1	2.69	11.9	0.616
23	367.5	0.2	21.0 6	79.3	0.72 5	2.62	11.4	0.62 9	2.62	12.2	0.584
24	367.5	0.4	20.8 9	79.8	0.71 5	2.40	10.7	0.61 1	2.40	11.4	0.576

Notes:  $w_0$ ,  $S_{r0}$ ,  $e_0$  are gravimetric water content, saturation degree and void ratio at initial state, respectively. The meaning of other letters is similar to that of  $w_0$ ,  $S_{r0}$  and  $e_0$ . The net confining pressure of specimen 12 is only imposed 0.36 MPa, attributed to the fact that output air pressure can only be stabilized at 0.76 MPa from the compressor.

## 2.4 Mercury Intrusion Porosimetry (MIP)

The representation small cubes ( $\sim 10 \times 10 \times 10$  mm), were trimmed from the center of specimens with targeted suctions. The cubes were then hydrated by freeze-drying technique with liquid nitrogen, to decrease negative influence on microstructure of specimen [24, 25]. The freeze-dried small cubes with different suctions were intruded mercury gradually by increasing loading step-by-step, and the curves of cumulative and differential intruded void ratio versus entrance pore diameter can be obtained.

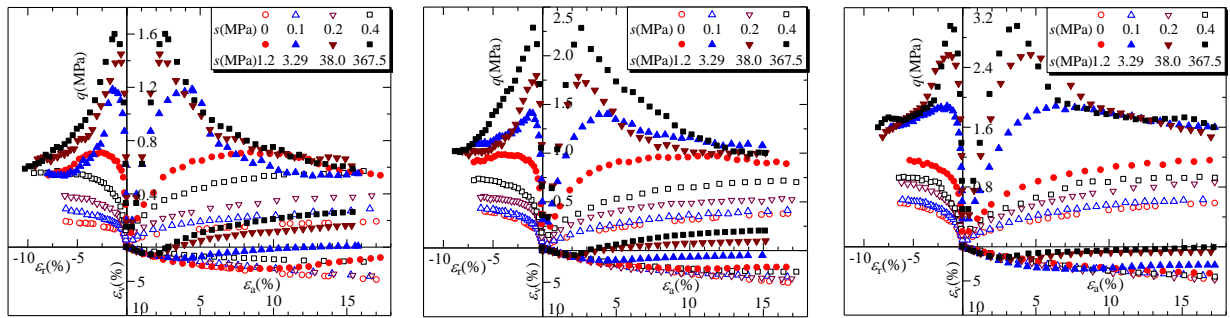
# III. TEST RESULTS AND DISCUSSION

## 3.1 Variation of strength with suction

Fig 4 shows obtained stress-strain-volumetric strain curves of undisturbed specimens under different suctions and net confining pressures. The letter  $q$  ( $=\sigma_{an}-\sigma_{rn}$ ) in the figure denotes the deviator stress,  $\sigma_{an}$  and  $\sigma_{rn}$  denote the net axial stress and net radial stress, respectively. In addition,  $\varepsilon_a$ ,  $\varepsilon_r$  and  $\varepsilon_v$  in the figure denote the axial strain, radial strain and volumetric strain, respectively.

Fig 4 demonstrates that the suction has great effect on the stress-strain curve of undisturbed specimen of the lateritic clay. Take the results of specimens sheared under net confining pressure of 0.1 MPa as an example (Fig 4a), it can be observed that the stress-strain curves are typical shear-contract and strain-hardening for specimens with low suctions ( $s \leq 0.5$  MPa). By contrast, the stress-strain curves are shear-dilatancy and strain-softening for specimens with high suctions ( $s \geq 1.5$  MPa). Moreover, higher peak strength, as well as more shear-dilatancy and strain-softening in stress-strain curves can be observed with an increase in suction. Correspondingly, the failure modes of specimens progressively change from the plastic failure with barrel deformation to the brittle failure with localized deformation with an increase in suction, and a single band pattern through the specimen can be observed in the failure specimens with medium to high suctions (Fig 5).





(a)  $\sigma_m=0.1MPa$

(b)  $\sigma_m=0.2MPa$

(c)  $\sigma_m=0.4MPa$

Fig 4: Stress-strain-volumetric strain curves with different suctions and net confining pressure



(a)  $s=0.2 MPa$

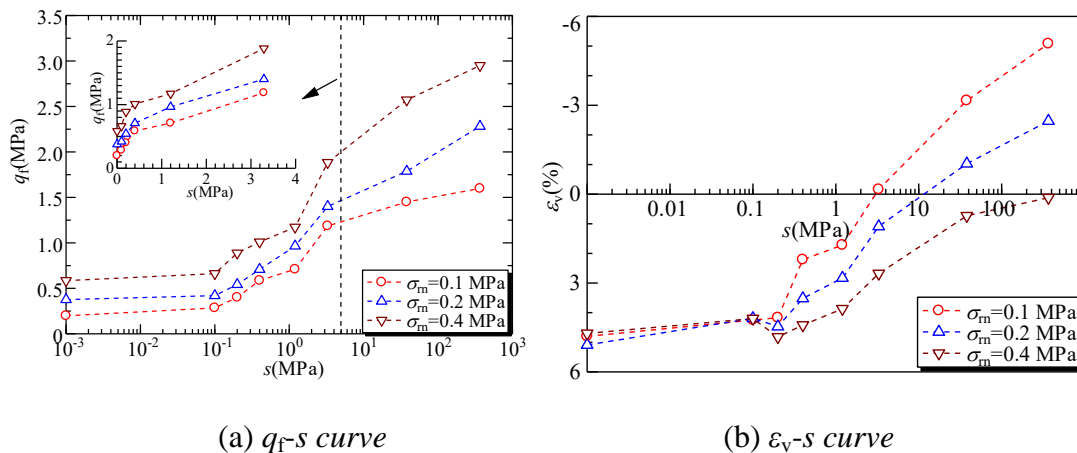


(b)  $s=1.2 MPa$



(c)  $s=367.5 MPa$

Fig 5: Failure modes of undisturbed specimens with different suctions ( $\sigma_m=0.1MPa$ )



(a)  $q_f-s$  curve

(b)  $\epsilon_v-s$  curve

Fig 6: Variations of peak strength and volumetric strain with suction for undisturbed specimens

Fig 6 illustrates the variations of peak strength and final volumetric strain with an increase in suction under different net confining pressures. It can be observed that the peak strength

continues to increase with an increase in suction, as shown in Fig 6(a). And that the increasing of peak strength with suction are linear and nonlinear in the semi-logarithmic coordinate for suction lower and higher than 1.2MPa, respectively. The variation of peak strength with suction is consistent to results obtained from silty clay or clay over a wide suction range [26, 27]. In addition, the peak strength also increases with an increase in net confining pressure, and that the influence of net confining pressure on peak strength is more significant for specimen with higher suction. Such as, the undisturbed specimens with the same suction, sheared at net confining pressure of 0.1 MPa and 0.4 MPa, respectively. The difference in peak strength is only 0.38 MPa for specimens with suction of 0.1 MPa. However, the difference in peak strength can reach to 1.34 MPa for specimens with suction of 367.5 MPa. The enlarged difference in peak strength is mainly caused by increasing difference in friction strength of lateritic clay, due to strengthening of friction between particles at high suctions [12].

Fig 6(b) demonstrates the variation of final volumetric strain with increasing suction. It can be observed that final volumetric strain changes gradually from contract to dilatancy with an increase in suction, and the maximum dilatancy can reach to 5.1%. It is worth noting that final volumetric strains obtained from specimens sheared at different net confining pressures, are almost the same for specimens with suction lower than 0.2 MPa. Therefore, the effect of net confining pressure on volumetric strain is limited for specimens with low suctions. In contrast, the shear-dilatancy obviously decreases with an increase in net confining pressure for specimens with medium to high suctions, and final volumetric strain of specimen changes from shear-dilatancy to shear-contract with an increase in net confining pressure. For example, the specimens with suction of 38.0 MPa, the shear-dilatancy is observed when the specimen sheared at net confining pressure of 0.1MPa, while the shear-contract is exhibited when the specimen sheared at net confining pressure of 0.4MPa. The above-mentioned results illustrate that the net confining pressure can obviously reduce the dilatancy of specimens with high suctions, while the effect on the final volumetric strain of specimens with low suctions is limited.

### 3.2 Variation of strength parameter with suction

The three Mohr circles can be drawn from the obtained shear strength of specimens with the same suction, sheared under three different net confining pressures. The cohesion and internal friction angle can be determined by drawing common tangent of Mohr circles, as shown in Fig 7. It is needed to emphasis that peak strength in the strain-softening stress-strain curve, is selected as the shear strength of specimens. Meanwhile, the deviator stress corresponding to the axial strain of 15% in the strain-hardening stress-strain curve, is selected as the shear strength of specimens. It needs to be interpreted that the determination of the

strength parameters (cohesion and internal friction angle) is not a major concern in this paper. As a result, only the results of specimens with suction of 3.29 MPa, sheared under different net confining pressures, are used as an example to illustrate the detailed method to determine the strength parameters (Fig7).

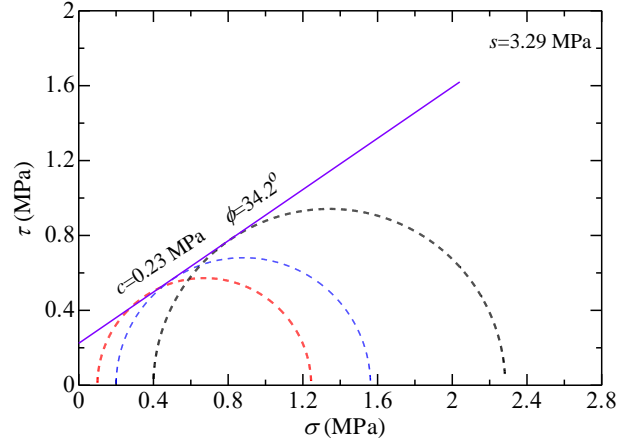


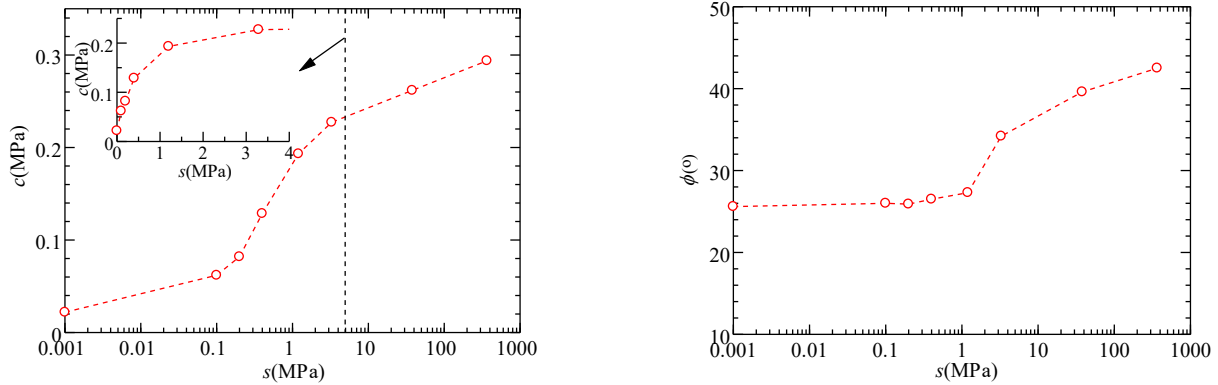
Fig 7: Determination of cohesion and internal friction angle

The variations of cohesion and internal friction angle with suction are shown in Fig 8(a)~8(b), respectively. It can be observed from Fig 8(a) that the cohesion continues to increase with an increase in suction. Moreover, the curve of cohesion versus suction in semi-logarithmic coordinate are linear and nonlinear in low to medium suctions ( $s \leq 1.5$  MPa) and high suctions ( $s > 1.5$  MPa), respectively. The obtained test result is consistent with the variation of cohesion with suction over a wide suction range, reported by Li et al. [12] and Shi et al. [20]. However, the variation of internal friction angle with suction is distinctly different, as shown in Fig 8(b). It shows that the internal friction angles are almost constant for specimens with low to medium suctions. On the contrary, the internal friction angle increases significantly with increasing suction in the high suction range. The variation of internal friction angle with suction is consistent to results obtained from the direct shear tests under constant gravimetric water content of lateritic clay [11]. It is worth emphasized that the variations of cohesion and internal friction angle with suction are obvious different, while the threshold suction (suction corresponding to abrupt change in variation tendency) is almost the same. It can be observed from Fig 8 that, the threshold suction of tested lateritic clay is about 1.2 MPa, based on the limited test results of undisturbed specimens with medium suctions.

### 3.3 Variation of PSDs with suction

Fig 9 illustrates the cumulative and differential curves of intruded void ratio versus entrance pore diameter, respectively. The  $e_m$  in Fig 9(a) is the cumulative intruded void ratio, measured from MIP, and symbols ( $\circ$ ,  $\triangle$  and  $\nabla$ ) in the  $e_m$  axis is the macro void ratio  $e$ , calculated from

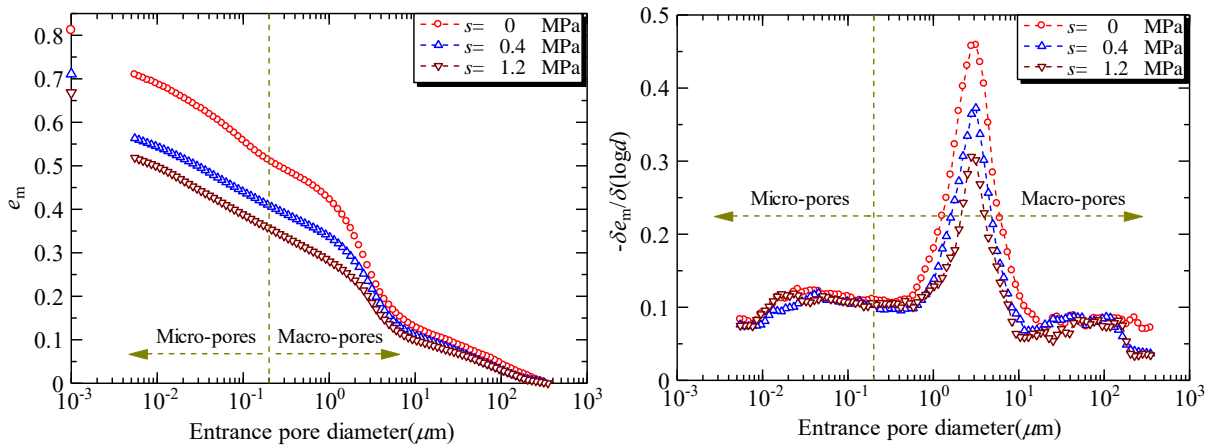
the measured volume and mass weight of specimens.



(a)  $c$ - $s$  curve

(b)  $\phi$ - $s$  curve

Fig 8: Variations of cohesion and internal friction angle with suction



(a) Cumulative intruded void ratio

(b) Differential intruded void ratio

Fig 9: Pore size distributions of undisturbed specimens with different suctions

Fig 9(a) shows that the cumulative intruded void ratio continues to increase, and it never flattens out with a decrease in the entrance pore diameter. The result indicates that there are numerous extra-small pores ( $d < 0.005 \mu\text{m}$ ) existing in used lateritic clay, which is not consistent to the MIP results obtained from other lateritic clays [5, 7, 10]. It can also be observed from Fig 9(a) that the cumulative intruded void ratio is only about 80% of the macro void ratio, caused by undetected extra-large pores ( $d > 350 \mu\text{m}$ ) and extra-small pores ( $d < 0.005 \mu\text{m}$ ). Nevertheless, it can be deduced that the difference in the cumulative intruded void ratio and macro void ratio, is mainly caused by numerous undetected extra-small pores, due to montmorillonite existing in the tested lateritic clay [28]. In addition, it can be observed from Fig 9(a) that the cumulative

intruded void ratio progressively decreases with an increase in suction, attributed to the reduction in void ratio of specimen. Moreover, the reduction in cumulative intruded void ratio is significant for the suction increases from 0 to 0.4 MPa, it is because that significant shrinkage of specimen are mainly occurred in normal shrinkage stage, due to significant water loss with small suction increment in low suctions.

It can be observed from Fig 9(b) that tested undisturbed lateritic clay exhibits unimodal PSDs, e.g. only one population of pores distributed between 0.5 to 10.0  $\mu\text{m}$ , as well as the peak entrance pore diameter is close to 3.0  $\mu\text{m}$ . The typical unimodal pattern of PSDs is consistent to the PSDs obtained from natural lateritic clay in Guilin, Guanxi province in China [5, 10]. Moreover, it can be observed from Fig 9(b) that the peak of intruded void ratio progressively reduces with an increase in suction, which is more obvious for suction increases from 0 to 0.4MPa. In addition, the progressively reduction in the frequency of pore size distribution with an increase in suction can also be observed in Fig 9(b), which demonstrates that the dominant pore size decreases with an increase in suction. It is worth noting that the peak entrance pore diameter is almost constant with an increase in suction, which indicates that the increasing suction can significant reduce the quantity of dominant pore size, while it has limited influence on the diameter of pores in dominant pore size distribution. The evolution of PSDs with suction is consistent to results obtained by Niu et al.[10], while it is obvious different to the evolution of PSDs with loading, obtained by Griffiths et al. [25] and Chen et al. [29].

According to the method to delimit macro- and micro-pores of clays with typical unimodal PSDs, suggested by Delage et al.[24], the delimiting diameter of tested lateritic clay can be selected as 0.17  $\mu\text{m}$  on the basis of the PSDs shown in Fig 9. Meanwhile, the delimiting diameter of macro- and micro-pores for other lateritic clays are about 0.3  $\mu\text{m}$ [4,7]. Consequently, 0.2  $\mu\text{m}$  is selected as the delimiting diameter for macro- and micro-pores of the tested lateritic clay in this study. Based on delimiting diameter of macro- and micro-pores, it can be observed from Fig 9(b) that t micro-pores in specimens with different suctions are almost coincident. Therefore, it can speculated that the suction only has great effect on macro-pores of clay, while the influence of suction on micro-pores of clay can be neglected.

#### **IV. MECHANISM ON THE VARIATION OF STRENGTH PARAMETERS**

It is well acknowledged that the hydraulic and mechanical behaviors are greatly related to its microstructure, and the evolution of hydro-mechanical behaviors can be well demonstrated upon the evolution of PSDs [5, 7, 30]. Thus, the mechanism on the variations of cohesion and internal friction angle with suction will be represented from the evolution of microstructure (PSDs) with suction.

The different variations of cohesion and internal friction angle with suction, as shown in Fig 8, can be attributed to different mechanism about suction effect on cohesion and internal friction angle. The cohesion of clay is mainly constituted by the interaction force, capillary attraction and bonding between soil particles, and it is significantly influenced by the distribution of capillary water in specimens. However, the internal friction angle is mainly determined by the thickness of bound water membrane, and it is mainly affected by the distribution of bound water in specimen [31]. According to the viewpoint that the capillary water is mainly distributed in macro-pores, while the bound water is mainly distributed in micro-pores of clay [32]. As a result, the variation tendency of cohesion and internal friction angle will change abruptly in the delimiting suction (suction corresponding to the delimiting diameter of macro- and micro-pores), from the viewpoint on evolution of microstructure with increasing suction in clay. Moreover, the delimiting suction should be consistent to the threshold suction deduced from curve of cohesion (or internal friction angle) versus suction in semi-logarithmic coordinate (Fig 8).

According to the mercury intrusion to porous medium, can be treated as the air injection in a saturated soil [5, 10, 33,34] in the drying procedure, and the suction can be deduced from pore diameter by Young-Laplace equation [35] as

$$s = u_a - u_w = 4\sigma_w \cos \alpha / d \quad (1)$$

where  $s$  is matric suction;  $u_a$  and  $u_w$  are the air and water pressures, respectively;  $\sigma_w$  is the surface pressure at the air/water interface, treated as 0.072 N/m at 20°C [22];  $\alpha$  is the contact angle between porous medium and water, and is assumed to be 0° in the calculation;  $d$  is the pore diameter.

The delimiting diameter for macro- and micro-pores of tested lateritic clay is 0.2  $\mu\text{m}$ , and the delimiting suction calculated from equation (1) is 1.44 MPa, which is close to the threshold suction ( $s=1.2$  MPa) obtained from triaxial compression tests. Due to the fact that small deviation in delimiting diameter of macro- and micro-pores, will result in great deviation in delimiting suction. Therefore, the delimiting suction is treated as the same to threshold suction in this paper, to illustrate the mechanism about the different change rules of strength parameters with increasing suction.

It can be observed from Fig 9(b) that the peak of intruded void ratio declines and the frequency of dominant pore size distribution reduces with an increase in suction gradually before the threshold suction. It indicates that the distance between particles progressively decreases, which is benefit to improve the interaction force of cohesion. On the other hand, the undisturbed specimens will be in unsaturated state when the suction exceeds the air-entry value

of clay, which will significantly improve the capillary force of cohesion. In addition, free iron oxide in clay will be transformed to crystalline iron oxide with the reduction of capillary water in clay, which is conducive to improve the bonding of cohesion. Due to the increasing of interaction force, capillary force and bonding, the cohesion increases linear with an increase in suction in semi-logarithmic coordinate before the threshold suction. However, when applied suction exceeds the threshold suction, the evolution of PSDs with suction will be weakened, and the increment of attraction force with an increase in suction, will be slowed down after the threshold suction. Moreover, the gravimetric water content is low when suction is larger than the threshold suction, the increasing of capillary force and bonding will also be reduced with an increase in suction. Consequently, despite the cohesion still increases with an increase in suction, it increases nonlinearly with suction in semi-logarithmic coordinate after the threshold suction.

The water in clay is expelled from macro- to micro-pores progressively with an increase in suction, as well as the bound water is mainly distributed in the micro-pores. The drained water is mainly capillary water distributed in the macro-pores, and the bound water distributed in micro-pores is not affected by progressively increasing suction before threshold suction. As a result, the internal friction angle is almost constant with an increase in suction before threshold suction, due to unchanged in the thickness of bound water membrane. However, when imposed suction exceeds threshold suction, the bound water distributed in micro-pores will be expelled gradually with an increase in suction. Correspondingly, the thickness of bound water membrane will be progressively thinned with increasing suction. Meanwhile, with the hardening of soil particles and enhancement of friction action between soil particles, the internal friction angle increases significantly with an increase in suction. Consequently, it can be speculated that the obvious increase in internal friction angle after threshold suction, can be attributed to the progressively thinned bound water membrane in the lateritic clay.

## **V. CONCLUSION**

In this paper, the effect of suction on the strength parameters on undisturbed lateritic clay, is discussed based on the variations of cohesion and internal friction angle with an increase in suction. In addition, the evolution of microstructure with suction, is used to illustrate the mechanism about different variations of strength parameters with increasing suction. The detailed conclusions are as follows.

The peak strength of undisturbed lateritic clay, progressively increases with an increase in the suction and net confining pressure, and it is more obvious for undisturbed specimen with high suction. In addition, the effect of net confining pressure can significantly reduce the



dilatancy of specimen with high suction, while the influence on the volumetric strain of specimen with low suction is limited.

The cohesion increases linear and nonlinear with suction in the semi-logarithmic coordinate before and after the threshold suction, respectively. On the contrary, the internal friction angle is almost constant with increasing suction before the threshold suction, while it increases significantly with an increase in suction after the threshold suction. In addition, the threshold suction, deduced from the triaxial compression tests on undisturbed specimen of lateritic clay, is about 1.2 MPa.

The undisturbed lateritic clay exhibits typical unimodal PSDs, and the peak entrance pore diameter of clay is close to 3.0  $\mu\text{m}$ . The peak of intruded void ratio declines, and the frequency of pore size distribution reduces with an increase in suction. In addition, the coincident distributions of micro-pores in specimens with different suctions, indicate that the suction has great effect on the macro-pores, while it has limited influence on the micro-pores of lateritic clay.

The distinct variations of strength parameters with suction can be attribute to the different mechanism about suction effect on cohesion and internal friction angle of clay. The cohesion is mainly influenced by the capillary water distributed in macro-pores. On the contrary, the internal friction angle is mainly affected by the bound water distributed in the micro-pores.

## ACKNOWLEDGEMENTS

This research was supported by Public Welfare Technology Research Projects of Zhejiang Province (No. LGG19E080002), Zhejiang Provincial Natural Science Foundation of China (LQ17E080012) and Joint Funds of Zhejiang Provincial Natural Science Foundation of China (LZY21D020001).

## REFERENCES

- [1] Gidigas MD (1972)“Mode of formation and geotechnical characteristics of laterite materials of Ghanan in relation to soil forming factors,” *Engineering Geology*, vol 6 no 2 pp 79-150
- [2] Miguel MG, Bonder BH (2012) “Soil-water characteristic curves obtained for a colluvial and lateritic soil profile considering the macro and micro porosity,” *Geotechnical and Geological Engineering*, vol 30 pp 1045-1420
- [3] Meshida EA (2006)“Highway failure over talc–tremolite schist terrain: a case study of the Ife to Ilesha highway, South Western Nigeria,” *Bulletin of Engineering Geology and the Environment*, vol 65 pp 457-461

- [4] Otálvaro I F, Neto M P C, Caicedo B (2015) “Compressibility and microstructure of compacted laterites,” *Transportation Geotechnics*, vol 5 pp 20-34
- [5] Sun DA, Gao Y, Zhou AN, et al. (2016) “Soil-water retention curves and microstructures of undisturbed and compacted Guilin lateritic clay,” *Bulletin of Engineering Geology and the Environment*, vol 75 pp 781-791
- [6] Chen YH, Li BY, Xu YT, et al. (2019) “Field study on the soil water characteristics of shallow layers on red clay slopes and its application in stability analysis,” *Arabian Journal for Science and Engineering*, vol 44 pp 5107-5116
- [7] Akinniyi C W W Ng, D B, Zhou C (2020) “Experimental study of the hydromechanical behaviour of a compacted lateritic sandy lean clay,” *Canadian Geotechnical Journal* vol 57 no 11 pp 1695-1703
- [8] Ma TH, Li CJ, Lu ZM, et al. (2015) “Rainfall intensity-duration thresholds for the initiation of landslides in Zhejiang Province, China,” *Geomorphology*, vol 245 pp 193-206
- [9] Filho OA, Fernandes MA (2019) “Landslide analysis of unsaturated soil slopes based on rainfall and matric suction data,” *Bulletin of Engineering Geology and the Environment*, vol 78 pp 4167-4185
- [10] Niu G, Sun DA, Shao LT, et al. (2021) “The water retention behaviours and pore size distributions of undisturbed and remoulded complete-intense weathering mudstone,” *European Journal of Environmental and Civil Engineering* vol 25 no 7 pp 1233-1250
- [11] Fu XH, Wei CF, Yan RT, et al. (2013) “Research on strength characteristics of unsaturated red clay,” *Rock and Soil Mechanics*. vol. 34, no. s2, pp. 204-209
- [12] Li LQ, Luo SX, Jiang H, et al. (2014) “Soil-water and shear strength characteristics of unsaturated red clay,” *Journal of Southwest Jiaotong University* vol 49 no 3 pp 393-399
- [13] Zhang ZL, Liang JJ, Huang Y, et al. (2018) “A study of the relationship between shear strength and microstructure of laterite under drying and wetting cycles,” *Hydrogeology and Engineering Geology*, vol 45 no 3 pp 78-85
- [14] Wang MW, Xu P, Li J, et al. (2015) “Microstructure and unsaturated geotechnical properties of net-like red soils in Xuancheng, China,” *Journal of Testing Evaluation*, vol 43 no 2 pp 385- 397
- [15] Gao Y, Sun DA, Zhu ZC, et al. (2019) “Hydromechanical behavior of unsaturated soil with different initial densities over a wide suction range,” *Acta Geotechnica*, vol 14 no 9 pp 417-428
- [16] Xu X, Cai GQ, Song ZY, et al. (2021) “Dilatancy characteristics and constitutive modelling of the unsaturated soil based on changes in the mass water content,” *Applied Sciences*, vol 11 pp 4859
- [17] Blatz J A, Cui Y J, Oldecop L (2008) “Vapour equilibrium and osmotic technique for suction control,” *Geotechnical and Geological Engineering*, vol 26 pp 661-673
- [18] Romero E, Gens A, Lloret A (1999) “Water permeability, water retention and microstructure of unsaturated compacted Boom clay,” *Engineering Geology*, vol. 54, no. 1-2, pp. 117-127
- [19] Gao Y, Sun DA (2017) “Soil-water retention behavior of compacted soil with different densities over a wide suction range and its prediction,” *Computes and Geotechnics*, vol. 91, pp. 17-25
- [20] Shi Y, Zhou L, Liu XW (2015) “Study on strength behavior of unsaturated laterite with GDS triaxial apparatus,” *Journal of Nanchang University (Engineering and Technology)* vol 37 no 4 pp 361-365
- [21] ASTM Standard D2487, “Standard practice for classification of soils for engineering purposes (Unified Soil Classification System),” ASTM International, West Conshohocken, Pennsylvania, U.S.A., 2011.
- [22] Fredlund DG, Rahardjo H (1993) “Soil mechanics for unsaturated soils,” New York: John Wiley and

Sons Inc

- [23] Greespan L (1977) "Humidity fixed points of binary saturated aqueous solutions," Research of the National Bureau of Standards, vol. 81A, no. 1, pp. 89-96
- [24] Delage P, Lefebvre G (1984) "Study of the structure of a sensitive Champlain clay and of its evolution during consolidation," *Canadian Geotechnical Journal* vol 21 no 1 pp 21-35
- [25] Griffiths FJ, Joshi RC (1989) "Change in pore size distribution due to consolidation of clays," *Géotechnique* vol 39 no 1 pp 159-167
- [26] Vanapalli SK, Wright A, Fredlund DG (2000) "Shear strength behavior of a silty soil over the suction range from 0 to 1,000,000 kPa," In: Proceedings of 53rd Canadian Geotechnical Conference, Montreal, QC, Canada 1161-1168
- [27] Zhang JR, Niu G, Li XC, et al. (2020) "Hydro-mechanical behavior of expansive soils with different dry densities over a wide suction range," *Acta Geotechnica*, vol 15 no 1, pp. 265-278,.
- [28] Alonso EE, Pinyoln M, Gens A (2013) "Compacted soil behavior: initial state, structure and constitutive modelling," *Géotechnique*, vol 63 no 6 pp 463-478
- [29] Chen B, Sun DA, Hu YS 2020 "Experimental study on strength characteristics of marine soft clays," *Marine Georesources and Geotechnology*, vol 38 no 5 pp 570-582
- [30] Simms PH, Yanful EK (2002) "Predicting soil-water characteristic curves of compacted plastic soils from measured pore-size distributions," *Géotechnique*, vol 52 no 4 pp 269-278
- [31] Deng JT, Wang JJ, Li RE, et al. (2016) "The strength characteristics of undisturbed loess under humidity-fied condition," *Journal of Arid Land Resources and Environment*, vol 30 no 1 pp 136-142
- [32] Dieudonne AC, Vecchia GD, Charlier R (2017) "Water retention model for compacted bentonites," *Canadian Geotechnical Journal* vol 54 no 7 pp 915-925
- [33] Hou XK, Qi SW, Li TL, et al. (2020) "Microstructure and soil-water retention behavior of compacted and intact silt loess," *Engineering Geology*, vol. 277 pp 105814
- [34] Wang YJ, Cui YJ, Tang AM (2015) "Effects of aggregate size on water retention capacity and microstructure of lime-treated silty soil," *Geotechnique Letters*, vol 5 no 4 pp 269-274
- [35] Diamond S (1970) "Pore size distribution in clays," *Clays and Clay Minerals*, vol. 18, no. 1, pp. 7-23